

# Quantum Geometry of Time-Reversal Symmetry Breaking in Flat-Band Superconductivity

Aaron Dunbrack,<sup>1</sup> Pauli Virtanen,<sup>1</sup> and Tero T. Heikkilä<sup>1</sup>

<sup>1</sup>*Department of Physics and Nanoscience Center, University of Jyväskylä,  
P.O. Box 35, FI-40014 University of Jyväskylä, Finland*

(Dated: March 20, 2025)

Several physical phenomena in superconductors, such as helical superconductivity and the diode effect, rely on breaking time-reversal symmetry. This symmetry-breaking is usually accounted for via the Lifshitz invariant, a contribution to the free energy which is linear in the phase gradient of the order parameter. In dispersive single-band superconductors with conventional pairing, the Lifshitz invariant can be computed from the asymmetries of the spectrum near the Fermi surface. We show that in multi-band superconductors, the quantum geometry also contributes to the Lifshitz invariant, and this is the dominant contribution when the low-energy bands are flat.

## I. INTRODUCTION

Historically, most theory on superconductors assumed dispersive bands and treated expansions about the Fermi energy centrally in their technique. In the past few years, however, there has been much focus on superconductivity in flat bands, where a Fermi surface description breaks down, motivated in part by the discovery of superconductivity in magic angle twisted bilayer graphene.

Central in these new descriptions is a dependence on *quantum geometry*: it describes the eigenvectors of the Hamiltonian rather than just the eigenvalues, and in particular on the variation of the eigenvectors with the crystal momentum  $k$ . Under suitable assumptions — notably including time-reversal symmetry — the superfluid weight in a flat band is directly proportional to the quantum metric, and it receives a contribution from the quantum metric even in a dispersive band [1–21]. What happens to these contributions without time-reversal symmetry has heretofore remained largely unexplored.

On general symmetry grounds, superconductors without time-reversal symmetry allow for several new phenomena, particularly when combined with inversion symmetry breaking. In terms of concrete applications, considerable attention has been paid to *diode effects*[22] where the critical current (above which the superconductivity breaks down) is higher in one direction of current flow than the other. A more abstract concept is *helical superconductivity*[23–26], where the superconducting order parameter takes on a phase modulation.

These effects can be quantified in terms of the *Lifshitz invariant*, [26–28] the coefficient of the contribution to the free energy that is linear in phase gradient. In other words, if  $\Psi$  is the superconducting order parameter, and one considers the part of free energy

$$F[\Psi(x)] = \vec{d} \cdot (i\Psi^\dagger \vec{\nabla} \Psi + h.c.) + \dots \quad (1)$$

then  $\vec{d}$  is the Lifshitz invariant. This is illustrated in Fig. 1.

The quantum geometric contributions to the Lifshitz invariant have been considered to some limited extent.

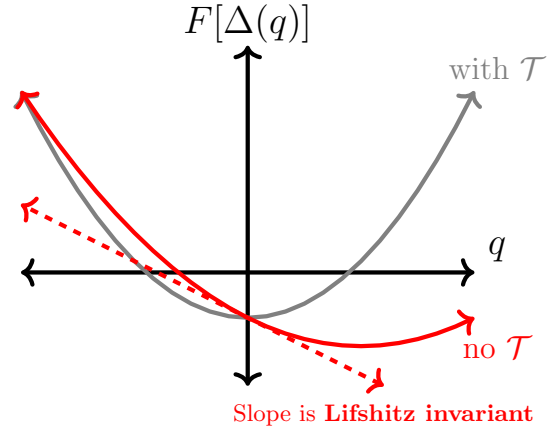


FIG. 1: The phase gradient  $q$  of the superconducting order parameter  $\Delta$  is odd under time-reversal symmetry  $\mathcal{T}$ . Accordingly, for time-reversal symmetric systems (gray), the free energy  $F$  is an even function of  $q$ , and thus is quadratic in phase gradients; this quadratic coefficient is the *superfluid stiffness*. However, if time-reversal symmetry is broken (red), then the free energy can have a linear coefficient called the *Lifshitz invariant*, which quantifies helical superconductivity, the  $\phi_0$  effect, and the superconducting diode effect.

However, perhaps the most central question remains unanswered: what are the consequences of breaking time-reversal symmetry in the quantum geometry itself? Ref. 29 breaks time-reversal by adding a suitable pairing term, and Ref. 30 considers quantum geometric effects when the spectrum breaks time-reversal symmetry, but both still preserve the symmetry at the level of the normal-state wavefunctions.

This paper resolves this problem for a wide range of Hamiltonians. We consider the case that time-reversal is broken only weakly, introducing a small parameter  $\alpha$  to characterize this perturbation, and use Ginzburg-Landau (GL) theory to compute the Lifshitz invariant, including explicit results for several models. These computations rely on a general notion of quantum geometry dependent

not only on  $k$  but also on the parameter  $\alpha$ , as explained in Appendix A.

In Section II, we outline the approach used to derive the GL coefficients (with details in Appendix B), including the requirements to use this approach, most importantly the ability to separate the states into high and low energy bands. Then, in Section III we compute the Lifshitz invariant in a simple example of a single-band superconductor with spin-orbit coupling. Finally, in Section IV, we provide an outlook for future theory development in this direction.

## II. METHODOLOGY

This section outlines the connection between quantum geometry and superconductivity. A more detailed algebraic derivation is presented in Appendix B; here, we highlight the ingredients that are unique to the time-reversal symmetry breaking case.

To make this connection, we make several simplifying assumptions about the model, with or without time-reversal symmetry:

- The spectrum must separate into low-energy and high-energy bands. The low-energy bands should be energy degenerate, and the high-energy bands should be widely gapped from these bands.
- The paired electrons should be time-reversed partners. This implies spin singlet pairing.
- Within the low-energy bands, pairing should be of uniform strength. This *uniform pairing condition* is the same as in the previous literature [1–3].

The assumptions on the spectrum are particularly noteworthy because they constrain the type of model under consideration. Accordingly, it is worth noting that these assumptions can be relaxed: provided the high-energy bands are always far from the Fermi surface and the low-energy bands are degenerate when near the Fermi surface, the methods presented here are still a good approximation. Being “far from” the Fermi surface in this context means differing by energies much larger than both the interaction strength and the temperature. The exact and approximate cases are compared in Fig. 2.

Some additional assumptions result from attacking the problem with perturbation theory. We characterize the time-reversal symmetry breaking by a small parameter  $\alpha$  which can be continuously tuned to a time-reversal symmetric Hamiltonian at  $\alpha = 0$ . For the full perturbative expansion to be valid, the above assumptions on the bandstructure and pairing should hold for all values of  $\alpha$ , although this requirement can be neglected for the linear-order-in- $\alpha$  contribution to the Lifshitz invariant.

We now proceed to outline the approach in more detail. In Section II A we review how quantum geometry contributes to superconductivity in the presence of time-reversal symmetry. Then, in Section II B, we lift this

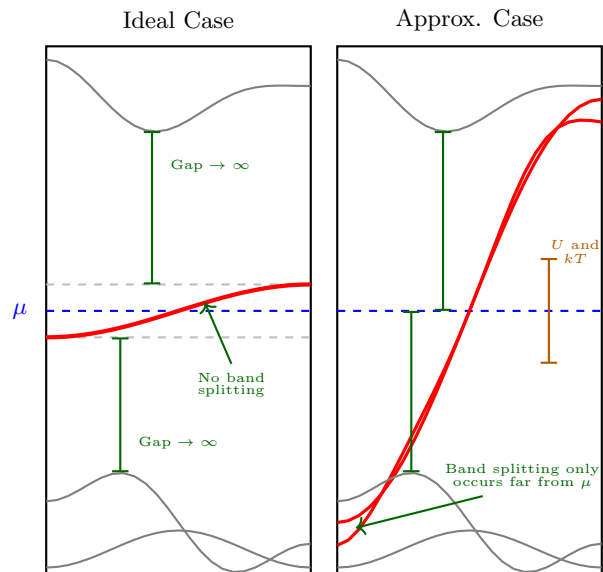


FIG. 2: To apply the techniques of Section II, the bandstructure needs to decompose into low-energy bands (red) near the Fermi level  $\mu$  (blue), and high-energy bands which are far enough from it to be integrated out. The approximations are illustrated in green: in the simplest case (left), the low-energy bands are degenerate with each other and isolated from other bands by a large gap. These requirements can be relaxed somewhat (right); the methods presented here are a good approximation provided both the high-energy bands and any energy-splittings between the low-energy bands are located far from the Fermi energy compared to  $U$  and  $kT$ .

assumption perturbatively and highlight how the same formalism can be extended. Finally, in Section II C, we provide a short algorithm to compute the lowest-order correction to the Lifshitz invariant in the perturbative parameter.

### A. Quantum geometry with time-reversal symmetry

As derived in Appendix B, the free energy expanded to quadratic order in the order parameter is given by

$$\Omega^{(2)} = \sum_q |\Delta_0(q)|^2 \left\{ U^{-1} N - \frac{T}{2} \sum_{\omega, k} \frac{\text{Tr}[P_k \mathcal{T} P_{-k-q} \mathcal{T}^{-1}]}{(i\omega - \epsilon(k))(-i\omega - \epsilon(-k-q))} \right\}, \quad (2)$$

where  $\Delta_0$  is the order parameter,  $U$  is the interaction strength,  $N$  is the number of low-energy bands,  $T$  is the temperature,  $P$  is the projector onto the low-energy

bands,  $\mathcal{T}$  is the time-reversal operator,  $\epsilon$  is the low-energy band dispersion, and  $\omega$  runs over Matsubara frequencies.

The portion of this equation that contributes to quantum geometry is the trace in the numerator of the second term. Because of time-reversal symmetry,  $\mathcal{T}P_{-k-q}\mathcal{T}^{-1} = P_{k+q}$ , and

$$\text{Tr}[P_k P_{k+q}] = 1 - g_{ij}q^i q^j + O(q^3) \quad (3)$$

where  $g_{ij}$  is the quantum metric, as written explicitly in Appendix A.

For the purposes of Ginzburg-Landau theory, the superfluid weight  $D^{ij}$  results from expanding the free energy as

$$\Omega^{(2)} = \sum_q |\Delta_0(q)|^2 \{a_0 + \frac{1}{2}D_{ij}q^i q^j + \dots\} \quad (4)$$

and therefore in a flat band where  $\epsilon(k) = 0$ , using the relation  $\sum_\omega \frac{T}{\omega^2} = \frac{1}{4T}$ , the superfluid weight is  $D_{ij} = \frac{1}{4T} \sum_k g_{ij}(k)$ .

In a dispersive band, one can add together contributions from the bandstructure (taking all  $q$ -derivatives in the energies, pretending the trace is 1) and from the quantum geometry (taking the quantum metric pretending a flat band) to get the total superfluid weight. Hence, the quantum geometry is relevant even without a perfectly flat band.

### B. Quantum geometry without time-reversal symmetry

We now consider removing the time-reversal symmetry at the perturbative level. Specifically, we assume the Hamiltonian of the system under consideration is continuously parameterized by a  $\mathcal{T}$ -breaking parameter  $\alpha$  as

$$H(\alpha) = H_0(\alpha^2) + \alpha H_1(\alpha^2) \quad (5)$$

where  $[\mathcal{T}, H_0] = 0 = \{\mathcal{T}, H_1\}$ . This decomposition of the Hamiltonian into its  $\mathcal{T}$ -symmetric and antisymmetric parts, which can always be done but demands a suitable definition of  $\alpha$ , ensures  $\mathcal{T}H(\alpha)\mathcal{T}^{-1} = H(-\alpha)$ . We denote the value of  $\alpha$  corresponding to a physical choice of Hamiltonian as  $\bar{\alpha}$ .

The resulting band energies and projectors now depend on  $\alpha$ , expressed in the notation  $\epsilon_\alpha(k)$  and  $P_{k,\alpha}$ . The reason for assuming this particular form of the Hamiltonian is to ensure the property  $\mathcal{T}P_{k,\alpha}\mathcal{T}^{-1} = P_{-k,-\alpha}$ , which follows naturally from  $\mathcal{T}H(\alpha)\mathcal{T}^{-1} = H(-\alpha)$ . Strictly speaking the latter condition is not required provided the former is met, but the decomposition is natural so little is lost by assuming this slightly stronger condition.

The derivation in Appendix B does not rely on time-reversal; only the final simplification of the trace in the previous section does. In this case, the trace term evaluates to

$$\text{Tr}[P_{k,\bar{\alpha}}\mathcal{T}P_{-k-q,\bar{\alpha}}\mathcal{T}^{-1}] = \text{Tr}[P_{k,\bar{\alpha}}P_{k+q,-\bar{\alpha}}] \quad (6)$$

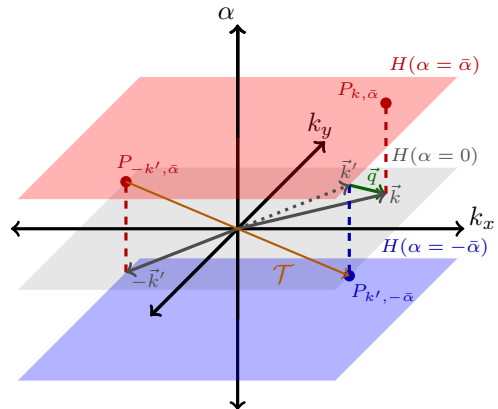


FIG. 3: Instead of evaluating the quantum geometry in the usual  $(k_x, k_y)$ -space, we evaluate it in  $(k_x, k_y, \alpha)$ -space, where  $\alpha$  is a perturbative  $\mathcal{T}$ -breaking parameter. The gray plane at  $\alpha = 0$  indicates the  $\mathcal{T}$ -symmetric case, the red plane indicates at finite  $\mathcal{T}$ -breaking  $\alpha = \bar{\alpha}$ , and the blue plane is the time-reverse of the red plane (by assumption on the definition of  $\alpha$ ). For  $\mathcal{T}$ -symmetric SCs,  $P_k$  and  $\mathcal{T}P_{-k'}\mathcal{T}^{-1}$  differ only in  $k$ -space (by momentum vector  $q$  from the gradient expansion), but without this symmetry, they also differ via  $\alpha \rightarrow -\alpha$ . Including this parameter in the quantum metric (and the quantum geometric coefficients of all higher-order corrections in  $q$ ) then accounts for this difference.

The two projectors can now be understood as separated both in momentum space and by their value of  $\alpha$ . In  $d$  dimensions, this can be understood as being separated in a  $d+1$ -dimensional space, as illustrated in Fig. 3.

The earlier analysis can straightforwardly be extended to this case provided one takes the more general perspective on quantum geometry outlined in Appendix A. For instance, to understand this expression to quadratic order in  $q$  and  $\bar{\alpha}$ , one can use the extended parameter space of Fig. 3 to express an extended quantum metric in terms of an index  $\mu$  that runs both over spatial indices  $i$  and an additional index  $\alpha$ ,

$$g_{\mu\nu} = \begin{bmatrix} g_{ij} & g_{i\alpha} \\ g_{\alpha j} & g_{\alpha\alpha} \end{bmatrix} = \text{Tr}[\partial_\mu P \partial_\nu P], \quad (7)$$

where  $g_{ij}$  is the usual quantum metric in  $k$ -space. It is worth noting at this stage that one could also introduce multiple  $\mathcal{T}$ -breaking parameters and view  $\alpha$  as a vector in some multidimensional space without changing the underlying derivation.

With this extended quantum metric and the corresponding difference of parameters of the projectors in this extended space,  $q^\mu = (q^i, 2\bar{\alpha})$ , the expansion to combined quadratic order in  $q$  and  $\alpha$  (i.e., the equivalent of Eq. (3))

is

$$\begin{aligned} \text{Tr}[P_k P_{k+q}] &= 1 - g_{\mu\nu} q^\mu q^\nu + \dots \\ &= (1 - 4\bar{\alpha}^2 g_{\alpha\alpha}) - 4\bar{\alpha} g_{i\alpha} q^i - g_{ij} q^i q^j + \dots \end{aligned} \quad (8)$$

The  $g_{i\alpha}$  term gives the Lifshitz invariant to linear order in  $\alpha$ , whereas  $g_{ij}$  is the usual contribution to superfluid weight. The  $g_{\alpha\alpha}$  term describes the reduction of critical temperature due to the time-reversal symmetry breaking: taking the simplest example, a flat band ( $\epsilon(k) = 0$ ), Eq. (2) reduces to

$$\Omega_{q=0}^{(2)} = |\Delta_0(0)|^2 \left\{ \frac{N}{U} - \frac{\sum_{\omega,k} \text{Tr}[P_{k,\alpha} P_{-k,-\alpha}]}{8T} \right\}. \quad (9)$$

Since  $g_{\alpha\alpha}$  would cause the second term to be less negative, it reduces the range of  $T$  where the expression as a whole is negative and where superconductivity is favored.

It might appear that the constant term would also give an estimate of the critical  $\bar{\alpha}$  at which superconductivity breaks down at  $T = 0$  (by analogy with critical magnetic field) as  $(4g_{\alpha\alpha})^{-1}$ , where the sign changes. However, terms that are higher order in  $\alpha$  cannot be neglected: the trace of a product of two projectors (generally: positive semidefinite matrices) is never negative, and only equals zero when  $P_{k,\alpha}$  and  $P_{-k,-\alpha}$  project onto orthogonal subspaces. Accordingly, there is no critical  $\bar{\alpha}$  beyond which the quantum geometric term implies superconductivity does not arise at any temperature.

Generally speaking, higher-order corrections in  $\alpha$  are similarly perfectly equivalent to higher-order corrections in  $q$  — the extension of  $q^i$  to  $q^\mu$  by the additional component  $2\bar{\alpha}$  works to all orders of the gradient expansion.

To include dispersive effects, one can expand both the trace and the dispersive part of a power series in  $q$  independently, then multiply said power series. Expressing this as

$$\Omega \sim (a_0^g + d_i^g q^i + g_{ij} q^i q^j + \dots)(a_0^\epsilon + d_i^\epsilon q^i + d_{ij}^\epsilon q^i q^j + \dots), \quad (10)$$

the Lifshitz invariant is essentially additive,

$$d_i \sim a_0^\epsilon d_i^g + a_0^g d_i^\epsilon, \quad (11)$$

whereas the superfluid weight now features a new cross term,

$$d_{ij} \sim a_0^\epsilon g_{ij} + a_0^g d_{ij}^\epsilon + (d_i^g d_j^\epsilon + [i \leftrightarrow j])/2, \quad (12)$$

which demands both  $\mathcal{T}$ -symmetry-breaking quantum geometry and nonzero dispersion. Note these expressions are before integrating over  $k$ , so in particular the cross-term in the superfluid weight can be nonzero even in the presence of inversion symmetry (where the Lifshitz invariant must vanish).

### C. Algorithm for the Lifshitz Invariant

In short, to compute the quantum geometric contribution to the Lifshitz invariant:

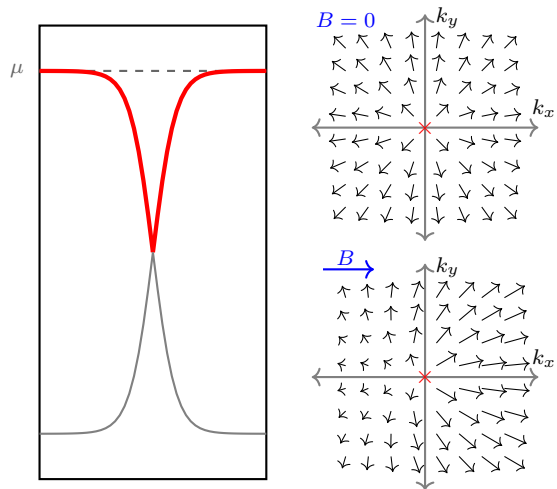


FIG. 4: (Left) The spectrum of a minimal two-band model for quantum geometric contributions to the Lifshitz invariant. Note that the Kramer's degeneracy is far from the chemical potential. (Right) The spin textures of Hamiltonian (13) in the flat band limit, with and without in-plane Zeeman field  $B$ . The red X denotes the singularity of the spin texture.

1. Decompose the Hamiltonian as  $H = H_0(\alpha^2) + \alpha H_1(\alpha^2)$  where  $[H_0, \mathcal{T}] = [H_1, \mathcal{T}] = 0$ .
2. Select low-energy bands and check the assumptions mentioned at the beginning of this section.
3. Compute the projector for the low-energy bands and the resulting extended quantum metric  $g_{\mu\nu}$ . If your atoms are not at high-symmetry positions, check that this is the minimal quantum metric; see Appendix B 1.
4. The quantum geometric contribution to the Lifshitz invariant can be computed using the off-diagonal components  $g_{i\alpha}$  of the extended quantum metric.
5. If this contribution vanishes, consider higher-order terms in  $\alpha$  and/or in  $q$ .

## III. MINIMAL MODEL

In this section, we construct a minimal model displaying quantum geometric contributions to the Lifshitz invariant — that is to say, one with only two bands from spin. Due to Kramer's degeneracy, it is impossible to separate these two bands by a wide gap at a time-reversal invariant  $k$ . However, if we set the chemical potential far from the energy of the Kramer's degeneracy, then this part of the Brillouin zone can be neglected, and the remainder of the Brillouin zone could be described by a well-gapped two-band model, as illustrated in Fig. 4.

A continuum model Hamiltonian describing this phenomenon in 2D is

$$H = v(k)k \cdot \sigma + B \cdot \sigma, \quad (13)$$

a combination of Rashba-like and Zeeman terms. A simple analytic function for  $v(k)$  is

$$v(k) = \frac{E_0 \tanh(|k|/k_0)}{|k|} \quad (14)$$

which is  $E_0/|k|$  unless  $|k| \lesssim k_0$ . In the limit  $k_0 \rightarrow 0$ , the dispersive contribution to the Lifshitz invariant scales like  $\frac{E_0}{k_0} \times k_0^2 \rightarrow 0$ , and the quantum geometric contribution from this portion of the spectrum similarly vanishes.

There remains the issue of large  $|k|$ , for which the integrated quantum geometry does not converge due to infinite  $k$ -space area in this continuum model. We therefore assume this Hamiltonian works up to some cutoff  $k_{\max}$ , beyond which the low-energy band diverges from  $\mu$  once more. This cutoff generates no quantum geometry and can be done symmetrically so as to add no extra Lifshitz invariant from the dispersion.

The additional dispersion both near  $k = 0$  and from the  $k_{\max}$  cutoff does offer a finite contribution to superfluid weight. However, in the large gap limit  $E_0/T \gg 1$ , this additional contribution approaches zero, so we neglect it.

The  $k_0 \rightarrow 0$  limit of this model is described by the Hamiltonian

$$H = (E_0 \hat{k} + B) \cdot \sigma, \quad (15)$$

which provides flat bands at  $B = 0$ . For algebraic simplicity, we now rescale to  $E_0 = 1$  and assume  $B = B_0 \hat{x}$ , leaving the only free parameter as the perturbative time-reversal-symmetry-breaking parameter  $B_0$ . Note that the system now has  $C_{2x}$  symmetry, so the only allowed Lifshitz invariant is in the  $x$  direction.

The projector of this system is

$$P = \frac{1}{2} \left[ 1 + \frac{(\cos(\theta_k) + B_0)\sigma_x + \sin(\theta_k)\sigma_y}{\sqrt{1 + 2B_0 \cos(\theta_k) + B_0^2}} \right] \quad (16)$$

with derivatives at  $B_0 = 0$  of

$$\partial_x P = \frac{\sin^2(\theta_k)\sigma_x - \sin(\theta_k)\cos(\theta_k)\sigma_y}{2|k|} \quad (17)$$

$$\partial_{B_0} P = \frac{\sin^2(\theta_k)\sigma_x - \sin(\theta_k)\cos(\theta_k)\sigma_y}{2} \quad (18)$$

The  $x$ -derivative blows up due to the nonanalytic behavior at  $k = 0$ , but in a way that converges to a finite answer in the integral over  $k$ .

Therefore, the quantum geometric contribution to the Lifshitz invariant is equal to

$$d_x^{(g)} = (T \sum_{\omega} \omega^{-2}) B_0 \int \text{Tr}[(\partial_x P)(\partial_{B_0} P)] d^2 k = \frac{\pi k_{\max} B_0}{32T E_0} \quad (19)$$

to first order in the perturbation  $B_0$ . For comparison, the dispersive contribution to the Lifshitz invariant, to leading order in  $B_0$ , is

$$d_x^{(\epsilon)} = -(T \sum_{\omega} \omega^{-3}) B_0 \int \frac{\sin^2(\theta_k)}{|k|} d^2 k = \frac{\pi k_{\max} B_0}{4T^2} \quad (20)$$

Note the different temperature dependence, arising from the different power of  $\omega$  in the Matsubara sum. When  $T$  is greater than the bandwidth of the individual bands, the  $T^{-1}$  behavior of the geometric part is generic, whereas the dispersive part will feature two terms proportional to  $T^{-2}$  and  $T^{-3}$ ; in this case the  $T^{-3}$  contribution vanishes because the time-reversal-symmetric bands are perfectly flat. While Ginzburg-Landau theory is only valid near  $T_c$ , this scaling should remain if one changes  $T_c$  by varying another parameter of the system, allowing the extraction of the quantum geometric part. For instance, in this case one could vary the chemical potential, although the temperature dependence will then be somewhat more complicated than simple scaling laws due to Fermi functions emerging from the Matsubara sum.

For this Hamiltonian, the geometric part is small compared to the dispersive part because we assume the temperature is much smaller than the gap,  $T \ll E_0$ . This naturally arises out of the fact that the only energy scale when  $B = 0$  is  $E_0$ , so the extra powers of  $T$  are necessarily powers of  $T/E_0$  by dimensional analysis, when working to linear order in  $B_0$ .

The resulting helical wavevector requires a computation of the superfluid weight, which diverges in the singular limit. If we instead integrate only away from the singularity, from  $k_0$  to  $k_{\max}$ , then

$$D_{xx} = (T \sum_{\omega} \omega^{-2}) \int \text{Tr}[(\partial_x P)^2] d^2 k = \frac{\pi L}{16T} \quad (21)$$

where  $L = \ln(k_{\max}/k_0)$  characterizes the singularity size relative to the size of the flat band. This implies a helical wavevector of

$$q_0 = \frac{d_x}{D_{xx}} = \frac{k_{\max} B_0}{2L} \left( \frac{1}{E_0} - \frac{8}{T} \right) \quad (22)$$

to leading order in  $B_0$ , where the first term is geometric and the second is dispersive.

It is worth noting that adding a term  $\epsilon(k)\sigma_0$  does not change the quantum geometric aspects of the problem, but does change the spectrum. Accordingly, one can write down a variant of this model with a purely quantum geometric Lifshitz invariant: the Hamiltonian

$$H = (E_0 \hat{k} + B) \cdot \sigma - [2E_0(\hat{k} \cdot B) + B^2]\sigma_0 \quad (23)$$

yields a vanishing dispersive part of the Lifshitz invariant, but the same quantum geometric part as the previous calculation. It also has the same superfluid weight, so the helical wavevector in this case would be

$$q_0 = \frac{k_{\max} B_0}{2E_0 L}, \quad (24)$$

independent of temperature.

#### IV. CONCLUSION

We have demonstrated how to compute quantities of interest within Ginzburg-Landau theory of superconductors in the presence of broken time-reversal symmetry at the level of the wavefunctions, provided the time-reversal symmetry breaking is characterized by a perturbative parameter  $\alpha$  and the Hamiltonian meets the other requirements outlined in Section II. The simplest of these quantities is the Lifshitz invariant, which can be computed to leading order in the perturbative symmetry-breaking parameter from the off-diagonal components of the extended quantum metric, defined as the quantum metric in the combined  $(k_x, k_y, \alpha)$  space.

We have then computed the Lifshitz invariant to leading order in these perturbative corrections in the simplest model of a superconductor with spin-orbit coupling. In so doing, we showed that the quantum geometric contribution to the Lifshitz invariant scales as  $T^{-1}$ , whereas the dispersive part of the quantum metric features contributions scaling as  $T^{-2}$  and  $T^{-3}$ . We also showed in

this example that it is possible to consider a case where the Lifshitz invariant originates entirely from quantum geometry.

It is possible to generalize the same approach for superconductors that weakly break time-reversal symmetry in other ways — for instance, with a pairing that deviates perturbatively from spin singlet. Additionally, while computing leading-order corrections to the superfluid weight is in principle equivalent to next-order corrections in the gradient expansion, an analogue of the minimal quantum metric condition has not been computed for these higher-order terms, so the details of this approach are also left for future analysis.

#### V. ACKNOWLEDGMENTS

This work was supported by the Keele and Jane and Aatos Erkko foundations as part of the SuperC collaboration and by the Finnish Quantum Flagship (project no. 210000621611). A.D. acknowledges useful conversations with Dathan Ault-McCoy regarding quantum geometry in parameter space.

- 
- [1] S. Peotta and P. Törmä, *Nature communications* **6**, 8944 (2015).
  - [2] L. Liang, T. I. Vanhala, S. Peotta, T. Siro, A. Harju, and P. Törmä, *Phys. Rev. B* **95**, 024515 (2017).
  - [3] K.-E. Huhtinen, J. Herzog-Arbeitman, A. Chew, B. A. Bernevig, and P. Törmä, *Phys. Rev. B* **106**, 014518 (2022).
  - [4] P. Törmä, L. Liang, and S. Peotta, *Phys. Rev. B* **98**, 220511 (2018).
  - [5] A. Julku, T. J. Peltonen, L. Liang, T. T. Heikkilä, and P. Törmä, *Phys. Rev. B* **101**, 060505 (2020).
  - [6] Z. Wang, G. Chaudhary, Q. Chen, and K. Levin, *Phys. Rev. B* **102**, 184504 (2020).
  - [7] T. Kitamura, A. Daido, and Y. Yanase, *Phys. Rev. B* **106**, 184507 (2022).
  - [8] M. Iskin, *Phys. Rev. A* **107**, 023313 (2023).
  - [9] M. Iskin, *Phys. Rev. B* **107**, 224505 (2023).
  - [10] G. Jiang and Y. Barlas, *Phys. Rev. B* **109**, 214518 (2024).
  - [11] M. Iskin, *Phys. Rev. B* **109**, 174508 (2024).
  - [12] A. Daido, T. Kitamura, and Y. Yanase, *Phys. Rev. B* **110**, 094505 (2024).
  - [13] S. A. Chen and K. T. Law, *Phys. Rev. Lett.* **132**, 026002 (2024).
  - [14] J.-A. Wang, M. Assili, and P. Kotetes, *Phys. Rev. Res.* **6**, L022053 (2024).
  - [15] M. Tam and S. Peotta, *Phys. Rev. Res.* **6**, 013256 (2024).
  - [16] J. Ahn and N. Nagaosa, *Phys. Rev. B* **104**, L100501 (2021).
  - [17] V. Peri, Z.-D. Song, B. A. Bernevig, and S. D. Huber, *Phys. Rev. Lett.* **126**, 027002 (2021).
  - [18] J. Herzog-Arbeitman, V. Peri, F. Schindler, S. D. Huber, and B. A. Bernevig, *Phys. Rev. Lett.* **128**, 087002 (2022).
  - [19] D. Porlles and W. Chen, *Phys. Rev. B* **108**, 094508 (2023).
  - [20] G. Jiang and Y. Barlas, *Phys. Rev. Lett.* **131**, 016002 (2023).
  - [21] W. Chen and W. Huang, *Science China Physics, Mechanics & Astronomy* **66**, 287212 (2023).
  - [22] M. Nadeem, M. S. Fuhrer, and X. Wang, *Nature Reviews Physics* **5**, 558 (2023).
  - [23] D. F. Agterberg and R. P. Kaur, *Phys. Rev. B* **75**, 064511 (2007).
  - [24] O. Dimitrova and M. V. Feigel'man, *Phys. Rev. B* **76**, 014522 (2007).
  - [25] A. Buzdin, *Phys. Rev. Lett.* **101**, 107005 (2008).
  - [26] D. F. Agterberg, in *Non-centrosymmetric superconductors*, Lecture notes in physics, Vol. 847, edited by E. Bauer and M. Sigrist (Springer, 2012) Chap. 5.
  - [27] V. P. Mineev and K. V. Samokhin, *Zh. Eksp. Teor. Fiz.* **105**, 747 (1994), [*Sov. Phys. JETP* 78, 401 (1994)].
  - [28] V. M. Edelstein, *J. Phys.: Condens. Matter* **8**, 339 (1996).
  - [29] T. Kitamura, S. Kanasugi, M. Chazono, and Y. Yanase, *Phys. Rev. B* **107**, 214513 (2023).
  - [30] J.-X. Hu, S. A. Chen, and K. T. Law, *Band-geometric origin of superconducting diode effect* (2024), arXiv:2403.01080 [cond-mat.supr-con].
  - [31] R. Cheng, *Quantum geometric tensor (Fubini-Study metric) in simple quantum system: A pedagogical introduction* (2013), arXiv:1012.1337 [quant-ph].
  - [32] A. Avdoshkin and F. K. Popov, *Physical Review B* **107**, 10.1103/physrevb.107.245136 (2023).
  - [33] Y.-Q. Ma, S. Chen, H. Fan, and W.-M. Liu, *Phys. Rev. B* **81**, 245129 (2010).

## Appendix A: Overview of quantum geometry

Broadly speaking, *quantum geometry* describes how the *eigenvectors* of some family of Hamiltonians varies as one varies some continuous parameter. In condensed matter physics, this parameter is traditionally the crystal quasimomentum  $k$ , but it is also used in atomic, molecular and optical physics, and quantum information contexts with the parameter being some adiabatically tunable knob (see, e.g., Ref. 31). The latter usage is in line with the typical introduction of Berry curvature in a graduate quantum mechanics course.

A subtle point is that the eigenvectors themselves are only determined up to phase (and up to unitary transformation when they are energy-degenerate). Accordingly, physical quantum geometric quantities must be invariant under these phase multiplications (generally gauge transformations). The usual method for avoiding such complications at a computational level is to express all quantities in terms of traces of projectors onto different states/bands.

This quantum geometry can be described completely[32] by the trace of triplets of projectors: if the energies  $E_n(x)$  and the traces  $\text{Tr}[P_n(x)P_m(y)P_l(z)]$  are known for all  $x, y$ , and  $z$  in the parameter space and  $n, m$ , and  $l$  indexing the eigenvalues of  $H$ , then one can reconstruct the full Hamiltonian  $H(x)$  up to a global unitary change of basis.

For simplicity, suppose now we are interested in only one band, allowing us to drop the  $nml$  indices and just write  $\text{Tr}[P(x)P(y)P(z)]$ . The quantities that arise most commonly in physical applications arise from the lowest nontrivial contributions to the Taylor expansion near  $x = y = z$ :

$$\begin{aligned} & \text{Tr}[P(x)P(x+\delta)P(x+\epsilon)] = \\ & 1 + \delta_\mu\epsilon_\nu \text{Tr}[P(\partial^\mu P)(\partial^\nu P)]/2 + O(\delta^2, \epsilon^2) \end{aligned} \quad (\text{A1})$$

This trace defines the *quantum geometric tensor*,

$$\mathcal{Q}^{\mu\nu} = 2 \text{Tr}[P(\partial^\mu P)(\partial^\nu P)], \quad (\text{A2})$$

a Hermitian matrix. The (symmetric) real part is called the *quantum metric*,

$$g^{\mu\nu} = 2 \text{Re}[\text{Tr}[P(\partial^\mu P)(\partial^\nu P)]] = \text{Tr}[(\partial^\mu P)(\partial^\nu P)], \quad (\text{A3})$$

and (antisymmetric) imaginary part gives the *Berry curvature*,

$$\Omega^{\mu\nu} = 4 \text{Im}[\text{Tr}[P(\partial^\mu P)(\partial^\nu P)]], \quad (\text{A4})$$

which in 2D is usually reduced from a 2-form to a pseudoscalar by contraction with the Levi-Civita tensor.

These terms then naturally lead to their derivatives,  $\partial_\mu g_{\nu\rho}$  and  $\partial_\mu \Omega_{\nu\rho}$ , called the *quantum metric dipole* and *Berry curvature dipole*, as well as higher moments. There are also higher-order terms in the expansion of the trace of projectors, most of which cannot be expressed in terms

of the quantum geometric tensor [32] but can still be relevant to physical quantities, including those discussed in this paper.

Finally, rather than considering only one particular band, one could consider the band indices  $nml$  as well. Preserving these indices generates the study of *non-Abelian quantum geometry*: the *non-Abelian quantum geometric tensor*[33] of some set of bands with projector  $P$  is defined by

$$\mathcal{Q}_{mn}^{\mu\nu} = 2 \text{Tr}[P(\partial^\mu P_m)(\partial^\nu P_n)], \quad (\text{A5})$$

with  $m, n$  running over band indices.

## Appendix B: From superconductivity to the quantum metric

In this appendix, we provide the full proof of the assertions made in Section II. We use the notation that  $ij$  run over orbitals within a unit cell (including different sublattices), whereas capital  $IJ$  to refer to the orbitals of individual lattice sites.

The GL free energy is

$$\Omega = U^{-1} \text{Tr}[\hat{\Delta}^\dagger \hat{\Delta}] - T \sum_{\omega} \text{Tr}[\ln(i\omega - H)] \quad (\text{B1})$$

Here, we assume a local interaction  $U$ , and  $\hat{\Delta}_{IJ} \propto \delta_{IJ}$  is a diagonal matrix. The BdG Hamiltonian  $H$  is

$$H = \begin{bmatrix} H_0 & \hat{\Delta} \\ \hat{\Delta}^\dagger & -H_0^T \end{bmatrix}, \quad (\text{B2})$$

and the trace  $\text{Tr}$  should be understood in real space as running over  $IJ$  indices. (The chemical potential  $\mu$  should be understood as having been absorbed into  $H_0$ .)

Expanding the trace log in  $\Delta$  and considering only the quadratic term in  $\Delta$  gives the contribution

$$\begin{aligned} \Omega^{(2)} = & U^{-1} \text{Tr}[\hat{\Delta}^\dagger \hat{\Delta}] \\ & + \frac{T}{2} \sum_{\omega} \text{Tr}[(i\omega - H_0)^{-1} \hat{\Delta} (i\omega + H_0^T)^{-1} \hat{\Delta}^\dagger]. \end{aligned} \quad (\text{B3})$$

This order of expansion is sufficient for studying the lowest-order gradient terms, the Lifshitz invariants and the superfluid weight.

We now make a series of assertions about the nature of superconductivity to reduce to the case where expressions in terms of quantum geometry are possible.

First, we take the superconductivity to be a spin singlet and write  $\hat{\Delta} = (i\sigma_y)\hat{\Delta}_{\sigma_0}$ . Using the relation

$$i\sigma_y(i\omega + H_0^T)(-i\sigma_y) = -\mathcal{T}(i\omega - H_0)\mathcal{T}^{-1} \quad (\text{B4})$$

and using the Green's function  $G = (i\omega - H_0)^{-1}$ , we can now write

$$\begin{aligned}\Omega^{(2)} = & U^{-1} \text{Tr} \left[ \hat{\Delta}_{\sigma_0}^\dagger \hat{\Delta}_{\sigma_0} \right] \\ & - \frac{T}{2} \sum_{\omega} \text{Tr} \left[ G \hat{\Delta}_{\sigma_0} \mathcal{T} G \mathcal{T}^{-1} \hat{\Delta}_{\sigma_0}^\dagger \right].\end{aligned}\quad (\text{B5})$$

We now Fourier transform this expression, but in so doing make an additional assertion about our system: we have translation symmetry. As a consequence, we can write

$$\begin{aligned}\hat{\Delta}_{\sigma_0, IJ} &= \sum_q \hat{\Delta}_{ij}(q) \delta_{r_I, r_J} e^{iq \cdot r_I} \\ G_{IJ} &= \sum_q G_{ij}(q) e^{iq \cdot (r_I - r_J)}\end{aligned}\quad (\text{B6})$$

whereupon

$$\begin{aligned}\Omega^{(2)} &= \sum_q U^{-1} \text{Tr} \left[ \hat{\Delta}(q) \hat{\Delta}(q)^\dagger \right] \\ & - \frac{T}{2} \sum_{\omega, k, q} \text{Tr} \left[ G(k) \hat{\Delta}(q) \mathcal{T} G(-k - q) \mathcal{T}^{-1} \hat{\Delta}(q)^\dagger \right].\end{aligned}\quad (\text{B7})$$

where now the traces should be understood as running over the indices  $ij$  only.

Next, we express  $G(k)$  in terms of projectors  $P_{k,n}$  and energies  $\epsilon_n(k)$  onto band  $n$  of  $H_0$  as

$$G(k) = \sum_n \frac{P_{k,n}}{i\omega - \epsilon_n(k)} \quad (\text{B8})$$

whereupon

$$\begin{aligned}\Omega^{(2)} &= \sum_q U^{-1} \text{Tr} \left[ \hat{\Delta}(q) \hat{\Delta}(q)^\dagger \right] \\ & - \frac{T}{2} \sum_{\omega, k, q, m, n} \frac{\text{Tr} \left[ P_{k,m} \hat{\Delta}(q) \mathcal{T} P_{-k-q,n} \mathcal{T}^{-1} \hat{\Delta}(q)^\dagger \right]}{(i\omega - \epsilon_m(k))(i\omega - \epsilon_n(-k - q))}.\end{aligned}\quad (\text{B9})$$

At this stage, we assert the separation of the spectrum into low and high-energy bands discussed in the main text and thereby approximate the expression by evaluating the  $m, n$  sums only over low-energy bands  $\bar{m}, \bar{n}$ , producing the low-energy Green's function

$$\bar{G} = \sum_{\bar{n}} \frac{P_{k, \bar{n}}}{i\omega - \epsilon_{\bar{n}}(k)} \quad (\text{B10})$$

Next, we assert the *uniform pairing condition*[2], which states that the pairing is the same magnitude in all low-energy bands. Algebraically, within the low-energy bands, this means

$$\hat{\Delta}(q) = \Delta_0(q) V(q) \quad (\text{B11})$$

where  $\Delta_0$  is a scalar representing the magnitude of pairing and  $V$  is some diagonal unitary matrix. Note that when time-reversal symmetry is broken, this is a stronger assumption than in time-reversal symmetric systems.

The free energy therefore simplifies to

$$\begin{aligned}\Omega^{(2)} &= \sum_q |\Delta_0(q)|^2 \left\{ U^{-1} N \right. \\ & \quad \left. - \frac{T}{2} \sum_{\omega, k} \text{Tr} \left[ \bar{G}(k) V(q) \mathcal{T} \bar{G}(-k - q) \mathcal{T}^{-1} V(q)^\dagger \right] \right\},\end{aligned}\quad (\text{B12})$$

where  $N$  is the number of bands.

For small  $q$  (and, for the time-reversal-symmetry breaking case discussed in the main text, small  $\alpha$ ),  $V(q)$  can be eliminated with a suitable choice of location for the origins of the orbitals, giving the *minimal quantum metric*. This is discussed at length in Appendix B1, so we presume this has been done and accordingly reduce the expression for the free energy to

$$\begin{aligned}\Omega^{(2)} &= \sum_q |\Delta_0(q)|^2 \left\{ U^{-1} N \right. \\ & \quad \left. - \frac{T}{2} \sum_{\omega, k} \text{Tr} \left[ \bar{G}(k) \mathcal{T} \bar{G}(-k - q) \mathcal{T}^{-1} \right] \right\} \\ &= \sum_q |\Delta_0(q)|^2 \left\{ U^{-1} N \right. \\ & \quad \left. - \frac{T}{2} \sum_{\omega, k, \bar{m}, \bar{n}} \frac{\text{Tr} \left[ P_{k, \bar{m}} \mathcal{T} P_{-k-q, \bar{n}} \mathcal{T}^{-1} \right]}{(i\omega - \epsilon_{\bar{m}}(k))(-i\omega - \epsilon_{\bar{n}}(-k - q))} \right\}.\end{aligned}\quad (\text{B13})$$

In the presence of time-reversal symmetry, the expression in the numerator describes non-Abelian quantum geometry, and an expansion in  $q$  reveals the quadratic term to be the non-Abelian quantum metric. In the absence of time-reversal symmetry, this can still be generalized to the augmented non-Abelian quantum metric in the same way.

However, one must still assume the uniform pairing condition, which would seem an unnatural constraint with many low-energy bands at varying energies. Most physical cases of the uniform pairing condition impose it by symmetry and, for the same reason, mandate that the corresponding bands be energy degenerate, such that  $\epsilon_{\bar{m}}(k) = \epsilon(k)$ .

This energetic constraint also simplifies our results here, and so we restrict ourselves to models with that property. In such a case, the sum over  $\bar{m}, \bar{n}$  can be performed explicitly by summing the projectors onto individual bands into the projector onto all low-energy bands  $P_k$ , therefore reducing the non-Abelian quantum metric to the Abelian one. This produces the resulting free en-

ergy

$$\Omega^{(2)} = \sum_q |\Delta_0(q)|^2 \left\{ U^{-1} N - \frac{T}{2} \sum_{\omega, k} \frac{\text{Tr}[P_k \mathcal{T} P_{-k-q} \mathcal{T}^{-1}]}{(i\omega - \epsilon(k))(-i\omega - \epsilon(-k-q))} \right\}, \quad (\text{B14})$$

as described in the main text in Eq. (2).

### 1. Minimal Quantum Metric

The  $V(q)$  are free parameters, and  $\Omega^{(2)}$  must be minimized with respect to this choice. However, it turns out that this minimization is perfectly equivalent to a different minimization problem that can be expressed purely in terms of quantum geometry, known as finding the minimal quantum metric. This fact was first identified in Ref. 3.

We begin, for simplicity, from Eq. (B12) and consider the simplest case of time-reversal-symmetric energy-degenerate bands. In this case, the interesting part of the calculation is the trace  $\text{Tr}[P_k V(q) P_{k+q} V(q)^\dagger]$ , which contributes to the free energy with a minus sign and so must be maximized.

Consider a particular  $q = q_0$  and select a vector of Hermitian diagonal matrices  $M$  such that  $V(q_0) = e^{iq_0 \cdot M}$ , which is always possible to do. Then, write  $\tilde{V}(q) = e^{iq \cdot M}$  for that choice of  $M$ . If we then define

$$\tilde{P}_k = \tilde{V}(k) P_k \tilde{V}(k)^\dagger \quad (\text{B15})$$

then

$$\text{Tr}[P_k V(q_0) P_{k+q_0} V(q_0)^\dagger] = \text{Tr}[\tilde{P}_k \tilde{P}_{k+q_0}] \quad (\text{B16})$$

Therefore, including maximization of the left-hand side trace over all  $V(q)$  is equivalent to maximizing the right-hand side trace over all  $\tilde{P}_k$ , i.e., over all changes of basis of the projectors of the form  $e^{ik \cdot M}$ . This can, in turn, be related to the locations of orbital centers, as shown in Ref. 3.

To quadratic order, this trace is  $1 - g_{ij} q^i q^j$ . Therefore, for small  $q$ , one wants to choose a basis that minimizes the  $q$ -direction eigenvalue of  $g_{ij}$ . As it turns out, it is possible to do this for every direction in  $k$ -space simultaneously by minimizing the trace of  $g_{ij}$ , producing what is called the *minimal quantum metric* [3].

Now, we lift the constraint of time-reversal symmetry. As discussed in the main text, at the perturbative level, one can view the breaking of time-reversal symmetry as adding a third, continuous parameter  $\alpha$  to  $k$ -space, whereupon the analogous trace is proportional to  $1 - g_{\mu\nu} q^\mu q^\nu$ , with  $\mu, \nu \in \{x, y, \alpha\}$ . Since the situation is entirely analogous once reduced to this extended quantum geometric, one can also assert that the appropriate choice of basis for the projectors  $\tilde{P}$  (which can now vary not only with  $k$  but also with  $\alpha$ ) is the one which minimizes the trace of the augmented quantum metric  $g_{\mu\nu}$ .